

**Experimental demonstration of composite adiabatic passage**

Daniel Schraft\* and Thomas Halfmann†

*Institut für Angewandte Physik, Technische Universität Darmstadt, Hochschulstraße 6, 64289 Darmstadt, Germany*

Genko T. Genov and Nikolay V. Vitanov

*Department of Physics, Sofia University, 5 James Bourchier Boulevard, 1164 Sofia, Bulgaria*

(Received 20 September 2013; published 10 December 2013)

We report an experimental demonstration of composite adiabatic passage (CAP) for robust and efficient manipulation of two-level systems. The technique represents an altered version of rapid adiabatic passage (RAP), driven by composite sequences of radiation pulses with appropriately chosen phases. We implement CAP with radio-frequency pulses to invert (i.e., to rephase) optically prepared spin coherences in a  $\text{Pr}^{3+}:\text{Y}_2\text{SiO}_5$  crystal. We perform systematic investigations of the efficiency of CAP and compare the results with conventional  $\pi$  pulses and RAP. The data clearly demonstrate the superior features of CAP with regard to robustness and efficiency, even under conditions of weakly fulfilled adiabaticity. The experimental demonstration of composite sequences to support adiabatic passage is of significant relevance whenever a high efficiency or robustness of coherent excitation processes need to be maintained, e.g., as required in quantum information technology.

DOI: [10.1103/PhysRevA.88.063406](https://doi.org/10.1103/PhysRevA.88.063406)

PACS number(s): 32.80.Qk, 42.50.Md, 82.56.Jn, 03.67.Ac

**I. INTRODUCTION**

Coherent control of quantum systems is a crucial requirement for most applications in quantum physics. Such control techniques are, e.g., based on adiabatic passage processes [1], which combine efficiency and robustness with regard to fluctuations in the experimental parameters. Basic and well-known adiabatic passage processes are rapid adiabatic passage (RAP) [2,3] and stimulated Raman adiabatic passage (STIRAP) [4]. RAP represents the simplest example of adiabatic passage, aiming at population inversion driven by a single radiation field in a two-level quantum system. In order to implement RAP, the carrier frequency of the radiation pulse is chirped across the transition frequency of the two-level system. Provided that the interaction strength (i.e., the Rabi frequency), the interaction time, and the chirp range are adequately adjusted and losses are sufficiently small during the interaction, the system is driven adiabatically from an initial ground to an excited state. We note that RAP also works in case of mixed states or arbitrary superpositions of two states. In this case, RAP inverts the population distribution of the quantum system. However, under realistic experimental conditions residual diabatic couplings always limit the inversion efficiency of RAP to values below 100%.

In order to improve the inversion efficiency and robustness of RAP, a recent theoretical proposal suggests combining adiabatic passage with the technique of composite pulses [5,6]. Theoretical ideas about and experiments on composite pulses [7] were originally developed in nuclear magnetic resonance (NMR). The basic idea of composite pulses is to replace excitations driven with a single radiation pulse by excitation with a sequence of pulses. The relative phases of the composite sequence pulse parts are chosen in such a way that the target state is optimized with respect to certain parameters. Thus, composite sequences exhibit solutions to an optimization

problem, with the phases of the single pulses as control parameters. The optimization may aim at arbitrary features, e.g., robustness with respect to variations in specific experimental parameters (i.e., broad operation bandwidth), higher selectivity with respect to experimental parameters (i.e., narrow operation bandwidth), or higher efficiency of the excitation process. The first, short composite pulse sequences for two-level systems in NMR were deduced from intuition and clever “guessing” of appropriate coherent excitation pathways on the Bloch sphere. Afterwards, complex numerical procedures (which often were only an elaborated way of guessing) were applied to determine longer sequences [7]. Recently, a straightforward, theoretical systematic approach to determine composite sequences of arbitrary order (i.e., number of pulses) for various optimization problems in coherent excitation of quantum systems with bound states was developed [5]. The new theoretical approach was applied to optimize the efficiency and operation bandwidth of RAP with a composite version of the adiabatic passage process, i.e., composite adiabatic passage (CAP). In this case, the single RAP pulse is replaced by a composite sequence of  $N$  single pulses with specifically designed relative phases. The appropriate choice of phases permits suppression or compensation of residual diabatic losses in RAP to any arbitrary order. This enables higher efficiencies as well as broader operation bandwidths, i.e., enhanced robustness of adiabatic passage.

In our work, we report the first experimental demonstration of CAP. For the experimental implementation and systematic studies we apply CAP to invert (or rephase, respectively) atomic coherences, i.e., coherent superpositions of two quantum states. We use the concept of stored light by electromagnetically induced transparency (EIT) [8] to optically write and later read the atomic coherences [9]. During the storage time between the write and the read processes, we apply CAP sequences to invert and rephase the coherences. The readout efficiency serves as a straightforward measure of the inversion (i.e., rephasing) efficiency. Our data clearly reveal the superior performance of CAP compared to conventional  $\pi$  pulses or RAP. The combination of adiabatic passage processes

\*daniel.schraft@physik.tu-darmstadt.de

†<http://www.iap.tu-darmstadt.de/nlq>

and composite sequences is of interest whenever the efficiency and robustness of excitation processes are limited by the range and stability of the system or the experimental parameters. As a prominent example, we note applications of adiabatic passage processes in quantum memories and quantum computing, which require such high efficiency and robustness.

## II. BACKGROUND

We consider a two-level quantum system of states  $|1\rangle$  and  $|2\rangle$  [see also Fig. 1 (left)], driven by a single radiation field. As we discuss below, in our specific experiment we deal with a radio-frequency (RF) transition between two hyperfine states. Thus, in the following we use the magnetic field strength  $B_{\text{RF}}$  to describe the radiation field and consider magnetic RF interactions. Nevertheless, all the arguments below hold true also for any type of transition and driving field. If the field is tuned to resonance and the decay of state  $|2\rangle$  is negligible during the interaction, the total population oscillates between the ground state and the excited state. The oscillation frequency is given by the Rabi frequency  $\Omega_{\text{RF}}(t) = \mu_{12}B_{\text{RF}}(t)/\hbar$ , with the magnetic transition dipole moment  $\mu_{12}$  and the magnetic field strength  $B_{\text{RF}}(t)$ . The two-level system experiences complete population inversion if the field matches the pulse area condition  $A = \int \Omega_{\text{RF}}(t)dt = \pi$ . This is the concept of diabatic population inversion by a resonant  $\pi$  pulse. If we consider the general case of detuned excitation by rectangular pulses, the pulse area condition must be modified and we use the effective Rabi frequency  $\Omega_{\text{eff}} = \sqrt{\Omega_{\text{RF}}^2 + \Delta^2}$ , involving the static detuning  $\Delta$ . We note that in an inhomogeneously broadened medium, inversion by  $\pi$  pulses only works perfectly for one specific frequency ensemble in the inhomogeneous manifold. For all other ensembles, the pulse area of the driving pulse deviates from  $\pi$ . A more detailed treatment shows that efficient inversion by  $\pi$  pulses requires the inhomogeneous bandwidth  $\Gamma_{\text{inh}}$  to be much smaller compared to the Rabi frequency  $\Omega_{\text{RF}}$  or the frequency bandwidth of the radiation pulse, i.e., the inverse of the pulse duration  $1/\tau$ . Thus, taking limitations in the available radiation field intensity and pulse duration into account, inversion by  $\pi$  pulses becomes

difficult, or even impossible, in media of large inhomogeneous broadening. Moreover,  $\pi$  pulses suffer from fluctuations, e.g., pulse intensity, pulse duration, temporal pulse shape, carrier frequency, and variations in the experimental parameters, e.g., spatial beam profile and inhomogeneous broadenings. Also, in this case the pulse area deviates from  $\pi$  and the population inversion becomes incomplete.

RAP overcomes the problems of  $\pi$  pulses. During the adiabatic passage process, the driving radiation field exhibits a (typically, but not necessarily, symmetric) chirp  $\Delta(t)$  across the transition frequency. Provided that the adiabaticity criteria are maintained, RAP efficiently inverts the population distribution, (almost) irrespective of the exact values of the experimental parameters. In particular, RAP permits inversion of inhomogeneously broadened media, provided the chirp range exceeds the inhomogeneous bandwidth [10,11], as long as two adiabaticity criteria are matched. The first adiabaticity criterion requires the total chirp range  $\Delta\nu = \int R(t)/(2\pi)dt$ , with the chirp rate  $R(t) = 2\pi d[\Delta(t)]/dt$ , to fulfill the condition  $2\pi\Delta\nu/\Omega_{\text{RF}} \gg 1$ ; i.e., the chirp range should exceed saturation broadening. The second adiabaticity criterion for RAP requires that  $\Omega_{\text{RF}}^2/R \gg 1$ ; i.e., the coupling should be sufficiently strong. Thus, the larger the experimentally accessible parameter range of the Rabi frequency, chirp range, and pulse duration (or chirp rate, respectively), the better we fulfill the adiabaticity criteria and the smaller the perturbing effects of residual diabatic couplings. However, as the range of usual experimental parameters (e.g., pulse intensities, chirp range, pulse durations) is always finite, diabatic couplings will generally limit the efficiency of RAP.

In order to reduce the effects of residual diabatic couplings and hence further improve RAP, a recently proposed concept suggests combining RAP with composite pulse sequences [5]. A composite sequence consists of  $N$  single pulses (i.e., sections) with different relative phases  $\phi_k$  for the respective pulse section  $k$ . The idea is to choose the phases in such a way that the basic effect of the single excitation pulse is maintained, while reducing the dependence on experimental imperfections. Based on a new general treatment of composite pulses, Torosov *et al.* [5] applied these ideas to optimize

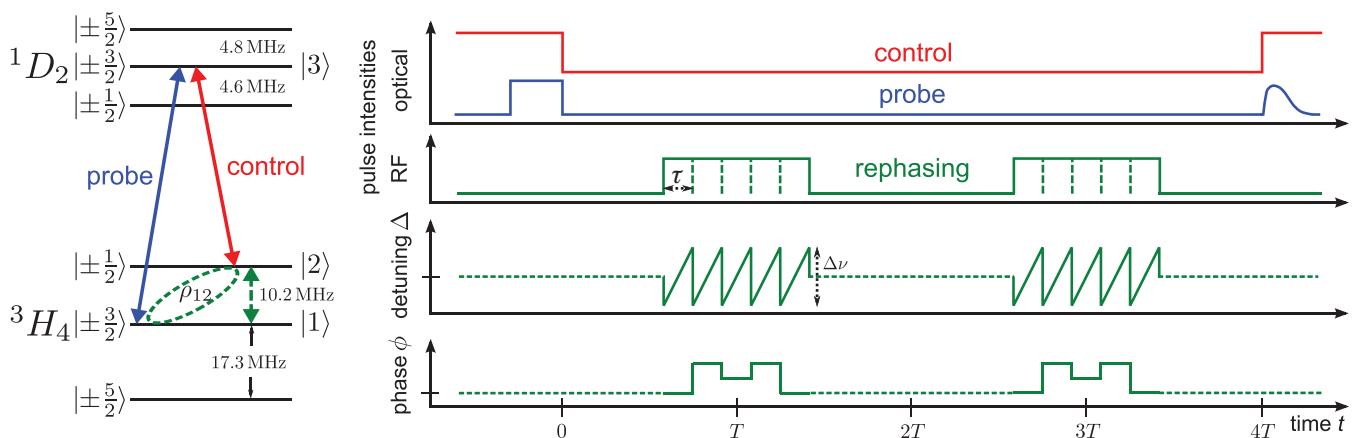


FIG. 1. (Color online) Left: Relevant hyperfine structure in  $\text{Pr}^{3+}:\text{Y}_2\text{SiO}_5$  and coupling scheme for optical excitation of atomic coherences by EIT [right (red) and left (blue) solid arrows] and rephasing by RF pulses [dashed (green) arrow]. Atomic coherence  $\rho_{12}$  is created between state  $|1\rangle$  and state  $|2\rangle$ . Right: Schematic pulse sequence for light storage by EIT, involving rephasing RF sequences. As an example, the scheme shows a CAP rephasing sequence with  $N = 5$  pulse sections, with a total chirp range  $\Delta\nu$  symmetric around  $\omega_{12}$ , and the variation of phase  $\phi$ .

TABLE I. Theoretically calculated phases  $\phi$  [5] of CAP sequences up to order  $N = 9$ .

$N$	Phase ( $\phi/\pi$ )							
3	0 2/3 0							
5	0 4/5 2/5 4/5 0							
7	0 6/7 4/7 8/7 4/7 6/7 0							
9	0 8/9 6/9 12/9 8/9 12/9 6/9 8/9 0							

RAP, which led to the concept of CAP. The sequences consist of an odd number,  $N = 2n + 1$ , of basic RAP pulses with relative phases  $\phi_k^{(N)}$ , derived from an analytic expression [5]. The phase sequence is symmetric, i.e.,  $\phi_1 = \phi_{2n+1}$ ,  $\phi_2 = \phi_{2n}$ ,  $\phi_3 = \phi_{2n-1}$ , ...,  $\phi_n = \phi_{n+2}$ . Because the global phase of the pulse sequence does not affect the inversion process, we set  $\phi_1 = \phi_{2n+1} = 0$ . Table I lists the phases  $\phi_k^{(N)}$  for CAP with  $N = 3, 5, 7$ , and 9 single RAP pulses. Figure 1 (right) schematically depicts an example of a CAP sequence with  $N = 5$ . As theoretically predicted, the CAP sequences permit the suppression of diabatic couplings in RAP. This can lead to enhanced robustness and higher efficiencies in a much broader range of experimental parameters.

Torosov *et al.* theoretically investigated CAP and RAP for population inversion of a two-state quantum system from an initial ground state to an excited state. Nevertheless, inversion by  $\pi$  pulses, RAP, and CAP works for any type of population distribution between two quantum states, e.g., also when initially some fraction of the population is in the excited state or when we deal with a coherent superposition of states. Thus, in our experiment we apply  $\pi$  pulses, RAP, and CAP to rephase atomic coherences in an inhomogeneously broadened medium. This is a very typical situation, e.g., in NMR, implementations of (quantum) memories by photon echo techniques or related approaches. In such an experiment, a broadband excitation process at time  $t = 0$  generates atomic coherences in the different frequency ensembles of an inhomogeneous manifold. Due to the inhomogeneity in the transition frequency (i.e., the oscillation period of the coherences), the atomic dipoles dephase. The application of a  $\pi$  pulse at time  $T$  realigns the atomic dipoles at time  $2T$ . This leads to the generation of an echo, i.e., the well-known Hahn echo [12].

The pulse energy of the echo is a direct measure of the rephasing efficiency. We note that often a second rephasing  $\pi$  pulse at time  $3T$  is applied in order to rephase the system a second time and, hence, restore also the original phase of the initial atomic coherence at time  $4T$ , based on the classical Carr-Purcell sequence [13]. Similarly to  $\pi$  pulses, rephasing is also possible by RAP [10,11]. Rephasing by RAP always requires a second pulse at time  $4T$ , if the Rabi frequency does not exceed the inhomogeneous bandwidth by much, i.e., if  $\Omega_{\text{RF}} \approx \Gamma_{\text{inh}}$  [14]. However, RAP offers enhanced robustness compared to  $\pi$  pulses. In an extension of RAP rephasing, we now apply CAP for rephasing of atomic coherences and compare its efficiency and robustness to those of  $\pi$  pulses and RAP.

### III. EXPERIMENTAL SETUP

In our experiment, we generate atomic coherences on a magnetic RF transition between hyperfine states  $|1\rangle$  and  $|2\rangle$ .

Preparation would be possible, e.g., by an RF  $\pi/2$  pulse. In our experiment, we write and read the atomic coherences optically via EIT [see Fig. 1 (left)]. A probe and a control laser pulse couple states  $|1\rangle$  and  $|2\rangle$  via an adiabatic Raman-type transition over an excited state  $|3\rangle$ . When we apply the two laser pulses in coincidence and match the falling edges of their temporal pulse profiles, a persistent atomic coherence between state  $|1\rangle$  and state  $|2\rangle$  is generated. With regard to the probe pulse, the latter is converted to the atomic coherence  $\rho_{12}$ . This phenomenon is called “stopped light” or “stored light” [8]. For optical readout after an arbitrary storage time we apply the control pulse again, which beats with the atomic coherence and thereby generates a signal pulse. Thus, EIT enables implementation of an optical memory (see, e.g., recent work in [15], and references therein). Also, in light storage by EIT, the atomic coherences experience dephasing during the storage time, i.e., between the write and the readout process. This strongly reduces the stored-light efficiency for storage times beyond the dephasing time  $T_{\text{deph}}$  of the medium. Thus, rephasing by RF excitation is required. The pulse energy of the retrieved signal pulse serves as a simple optical measure for the rephasing efficiency of  $\pi$  pulses, RAP, and CAP sequences. We perform the experiments in a  $\text{Pr}^{3+}:\text{Y}_2\text{SiO}_5$  crystal with a length of  $l = 3.2$  mm and a doping concentration of 0.02 at.% praseodymium. Figure 1 (left) shows the level structure of the  $\text{Pr}^{3+}$  ions in the host lattice. The scheme consists of an electronic ground state  $^3\text{H}_4$  and an excited state  $^1\text{D}_2$ . Each electronic state involves three doubly degenerate hyperfine levels, labeled by the magnetic quantum number  $m_I = \pm\frac{1}{2}, \pm\frac{3}{2}, \pm\frac{5}{2}$ . The population lifetime of the ground-state hyperfine levels is  $T_1 = 100$  s, while the excited-state hyperfine levels exhibit the much shorter population lifetime of  $T_1^* \approx 164$   $\mu\text{s}$ . Lattice defects in the host crystal cause variations of the local electric field. This leads to an inhomogeneous broadening of the optical transitions by several gigahertz. The optical probe field couples states  $^3\text{H}_4|\pm\frac{3}{2}\rangle \equiv |1\rangle$  and  $^1\text{D}_2|\pm\frac{3}{2}\rangle \equiv |3\rangle$ . The optical control field drives the transition between state  $^3\text{H}_4|\pm\frac{1}{2}\rangle \equiv |2\rangle$  and state  $^1\text{D}_2|\pm\frac{3}{2}\rangle \equiv |3\rangle$ . To prepare this  $\Lambda$ -type coupling in a single-frequency ensemble of  $\text{Pr}^{3+}$  ions an optical pumping sequence prior to the light storage experiments is required. For details on appropriate optical preparation sequences in  $\text{Pr}^{3+}:\text{Y}_2\text{SiO}_5$ , see [16] and [17]. The RF rephasing pulses couple the hyperfine transition  $|1\rangle \leftrightarrow |2\rangle$ . The inhomogeneous broadening of the RF transition is of the order of  $\Gamma_{\text{inh}} \approx 30$  kHz [17]. This corresponds to a dephasing time of  $T_{\text{deph}} = 1/(\pi\Gamma_{\text{inh}}) \approx 10$   $\mu\text{s}$ . The coherence lifetime of the RF transition, limited by stochastic phase perturbations, is  $T_2 = 500$   $\mu\text{s}$ . A single longitudinal-mode, continuous-wave, dye laser (SIRAH Matisse DX) provides radiation at  $\lambda = 605.98$  nm with an FWHM bandwidth of about 100 kHz on a time scale of 100 ms, limited by frequency jitter. The laser radiation is split into a weak probe beam (maximal power,  $P_p \approx 1.5$  mW) and a stronger control beam (maximal power,  $P_c \approx 100$  mW). The beams propagate through acousto-optic modulators (Brimrose BRI-TEF-80-50-.606) in a double-pass configuration. This setup allows full control of the temporal intensity and frequency profiles of the optical pulses, with a temporal resolution well below 100 ns. The control and probe beams are overlapped inside the crystal with beam diameters (FWHM of intensity) of  $\varnothing_c = 300$   $\mu\text{m}$  and

$\varnothing_P = 120 \mu\text{m}$ . This leads to maximal peak Rabi frequencies of  $\Omega_C = 2\pi \times 518 \text{ kHz}$  and  $\Omega_P = 2\pi \times 196 \text{ kHz}$  for the optical transitions required for light storage. A liquid helium cryostat (Janis Research ST-100) cools the medium to 4 K to suppress interactions with phonons. A pair of coils in a Helmholtz-like configuration, placed inside the cryostat around the crystal, serves to provide the RF radiation to drive the transition between state  $|1\rangle$  and state  $|2\rangle$ . The RF pulses are written by an arbitrary waveform generator (Tektronix AWG 5014) and pass a power amplifier (EM Power 1028-BBM 1C3KAJ) afterwards. At a sampling rate of 1.2 GS/s the AWG enables full control of the temporal intensity, frequency, and phase profiles of the RF pulse sequences. The phase resolution is approx.  $3 \times 10^{-4} \pi$ . To ensure optimal power transmission between the amplifier and the RF coils, we apply a single-frequency impedance matching circuit. The setup enables Rabi frequencies of up to  $\Omega_{\text{RF}} \approx 2\pi \times 145 \text{ kHz}$  for the RF transition. Bandwidth limitations of the electronic network lead to a minimal rise time of  $\tau_{\text{rise}} \approx 1 \mu\text{s}$  in the generated RF pulses.

For the experiments on RAP and CAP, we apply RF rephasing sequences with linear frequency chirps. We use CAP sequences with up to nine single RF pulses and a total duration of up to  $200 \mu\text{s}$ . The schematic pulse sequence for EIT light storage and the RF rephasing pulse by RAP or CAP are depicted in Fig. 1 (right). The optical probe and control (write) pulses generate a coherence between state  $|1\rangle$  and state  $|2\rangle$ . We read out the coherence by a control (read) pulse after a storage time of  $\Delta t = 600 \mu\text{s}$ , i.e., well beyond the dephasing time but still in the range of the coherence time  $T_2$ , to generate a signal pulse. During the storage time  $\Delta t$  we rephase the coherence twice with RF pulses at  $T = 150 \mu\text{s}$  and  $3T = 450 \mu\text{s}$ . The rephasing sequence with two RF pulses inverts the system twice and hence recovers the initial coherence's phase and population distribution. To compare the performance of RAP and CAP, we maintain all experimental parameters of the optical storage and retrieval process fixed, while we systematically vary the parameters of the rephasing sequences. We measure the pulse energy in the retrieved signal with a photodiode (Newfocus Model 2051). From this signal we calculate the stored-light efficiency  $\eta$  with respect to the initial probe pulse energy. This serves as a measure to evaluate the performance of different strategies to invert (or to rephase) a two-level quantum system, e.g., with  $\pi$  pulses, RAP, or CAP sequences.

#### IV. EXPERIMENTAL RESULTS

In the following, we systematically investigate the performance of CAP sequences for rephasing in light storage. We compare the results with rephasing by  $\pi$  pulses and RAP. We note that in the following sections we use the terms “stored-light efficiency” and “rephasing efficiency” synonymously. As in our specific experiment we change only the experimental parameters of the rephasing RF pulses; the stored-light efficiency depends only on the rephasing efficiency of the RF pulses. We note that the absolute stored-light efficiency is rather low (i.e., in the range of 1%–2%), as we did not optimize our setup for optimal EIT light storage. However, the aim here is a systematic comparison of inversion by  $\pi$  pulses, RAP, and

CAP, therefore only the relative differences in the stored-light efficiencies matter.

##### A. CAP efficiency vs pulse duration

In the first measurement, we investigate the dependence of the stored-light efficiency (i.e., the rephasing efficiency) vs the duration of the driving RF pulses. We apply pulses with rectangular temporal profiles, at the maximal power permitted by our RF source. The maximal Rabi frequency of the RF pulses is  $\Omega_{\text{RF}} \approx 2\pi \times 145 \text{ kHz}$ . This enables us to use  $\pi$  pulses with short durations of a few microseconds. We note that short rectangular pulse shapes are a good choice for inversion or rephasing by  $\pi$  pulses, due to the relatively large bandwidth, which, e.g., can cover fluctuations of the carrier frequency or inhomogeneous broadenings of the medium. For adiabatic rephasing processes (i.e., CAP and RAP), smoother temporal pulse shapes (e.g., Gaussian or sech) would be favorable. Thus, comparison of inversion or rephasing performances by CAP or RAP against  $\pi$  pulses is very conservative with regard to the latter. Moreover, we note that rectangular pulses enable us to clearly separate the single-pulse sections of a CAP sequence. We performed the measurement of RAP and CAP for two chirp ranges, i.e.,  $\Delta\nu = 600$  and  $900 \text{ kHz}$ . In both cases, this results in fairly fulfilled adiabaticity criteria (see below).

Figure 2(a) shows the stored-light efficiency  $\eta$  vs the single-pulse duration  $\tau$  for  $\pi$  pulses, RAP, and CAP sequences of  $N = 3, 5, 7$ , and  $9$  single pulses for a chirp range of  $\Delta\nu = 600 \text{ kHz}$ . The relative phases in the CAP sequences are the same as theoretically calculated in [5] and listed in Table I. We note that for CAP we must distinguish between single-pulse duration and total pulse duration. A  $\pi$  pulse or RAP rephasing process contains only a single pulse. Thus, there is no difference between the single-pulse and the total pulse duration. On the other hand, a CAP sequence contains  $N$  pulses. Hence, for CAP the total pulse duration is  $N$  times the single-pulse duration. This is a straightforward definition, because RAP can be understood as a CAP sequence of order  $N = 1$ .

The performance of RAP (and CAP) is mainly determined by the adiabaticity criteria. A fair and meaningful comparison of RAP and CAP requires identical adiabaticity in both cases. Therefore, we now compare  $\pi$  pulses, RAP, and CAP at the same single-pulse duration. This yields identical adiabaticity conditions for the single adiabatic processes in RAP and CAP, i.e., the same interaction time, pulse intensity, and chirp rate. We note that when we consider an imperfect RAP process (e.g., suffering from residual diabatic couplings), a conventional sequence of  $N$  RAP processes would yield an even worse performance due to the multiplied effect of the perturbations. Thus, comparing an arbitrary CAP sequence of  $N$  single pulses (each with duration  $\tau$ ) with the corresponding single RAP pulse (also of duration  $\tau$ ) is a very conservative approach to evaluate the performance of CAP.

As Fig. 2(a) shows, the best  $\pi$  pulse rephasing efficiencies are obtained for a pulse duration of about  $3.4 \mu\text{s}$  [see black crosses in Fig. 2(a)]. This yields a stored-light efficiency of approx. 1.15%. Already a small variation in the pulse duration (i.e., the pulse area) leads to a large decrease in the stored-light

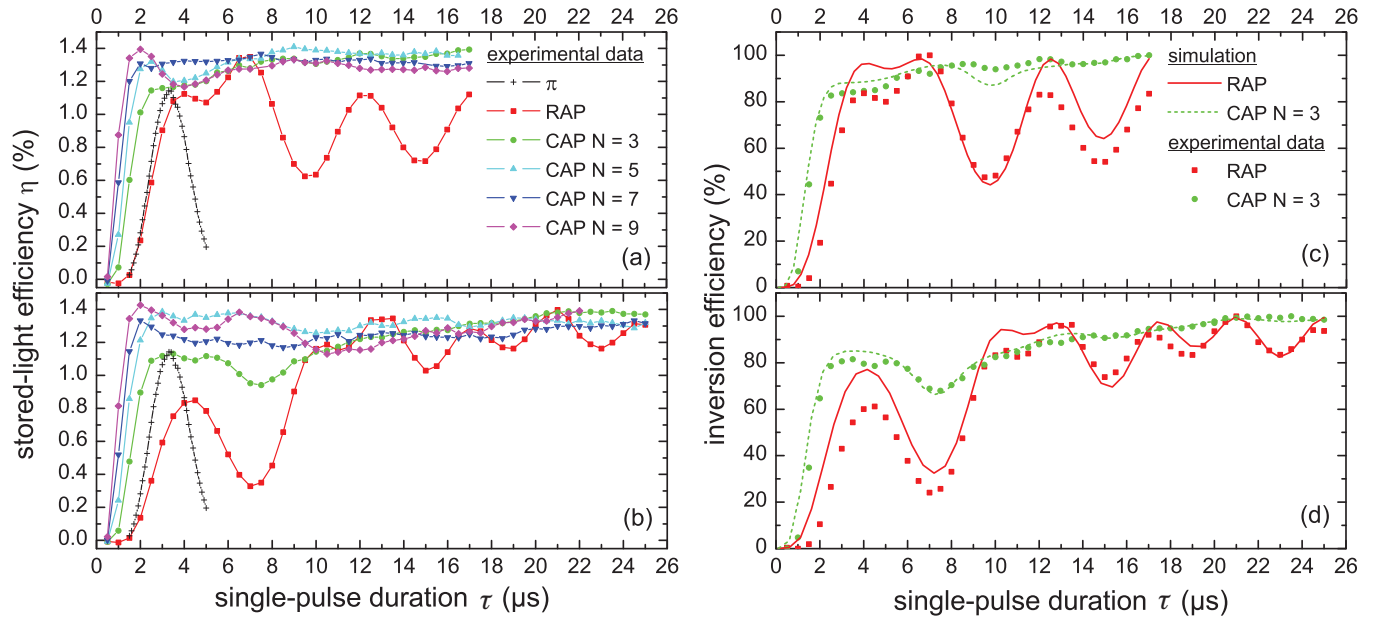


FIG. 2. (Color online) Stored-light efficiency  $\eta$  due to rephasing by  $\pi$  pulses, RAP, and CAP vs single-pulse duration  $\tau$ . In the case of CAP we apply sequences of  $N = 3, 5, 7,$  and  $9$  single pulses. The Rabi frequency is  $\Omega_{\text{RF}} = 2\pi \times 145$  kHz. All pulses have a rectangular temporal shape of the intensity. (a) Experimental data with a chirp range (for RAP and CAP) of  $\Delta\nu = 600$  kHz. (b) Experimental data with a chirp range (for RAP and CAP) of  $\Delta\nu = 900$  kHz. Lines along the experimental data are guides for the eye only. (c, d) Simulations (solid/dotted lines) and corresponding experimental data (filled squares, RAP; filled circles, CAP) at chirp ranges of (c)  $\Delta\nu = 600$  kHz and (d)  $\Delta\nu = 900$  kHz. We note that in the simulations we depict the calculated inversion efficiency instead of the measured stored-light efficiency (which both are proportional to each other).

efficiency, i.e., rephasing efficiency. As expected for diabatic interactions, the operation range of  $\pi$  pulses is very small. The situation improves for rephasing by RAP [see filled (red) squares in Fig. 2(a)]. For pulse durations in the interval roughly between  $4$  and  $8$   $\mu\text{s}$  we get a high rephasing efficiency, i.e., as high as or higher than the maximal efficiency for  $\pi$  pulses. The maximal efficiency is obtained at a pulse duration of  $7$   $\mu\text{s}$ . Compared to  $\pi$ -pulse rephasing, the maximal efficiency in RAP rephasing improved by  $13\%$ .

We note that RAP rephasing shows some pronounced oscillations in the efficiency. This is due to the fact that we only fairly fulfill the adiabaticity criteria for RAP (see Sec. II) in our experiment. The first adiabaticity criterion requires a large chirp range compared to the Rabi frequency. In our case, the ratio of chirp range  $\Delta\nu = 600$  kHz to Rabi frequency  $\Omega_{\text{RF}} = 2\pi \times 145$  kHz (in units of circular frequencies) is  $2\pi \Delta\nu / \Omega_{\text{RF}} = 4.14$ . This is larger, but not very much larger, than  $1$ . Moreover, we must also consider the second adiabaticity criterion for RAP. As we performed our measurements at fixed chirp ranges  $\Delta\nu$ , the chirp rate  $R$  depends on the single-pulse duration  $\tau$ . For the interval of pulse durations depicted in Fig. 2(a), the adiabaticity criterion  $\Omega_{\text{RF}}^2 / R$  varies between  $0.11$  and  $3.74$  for pulse durations of between  $0.5$  and  $17$   $\mu\text{s}$ . Thus, the second adiabaticity criterion is not well fulfilled, in particular, for shorter pulse durations. The deviations from perfect adiabaticity yield residual diabatic couplings, mirrored by the oscillating RAP rephasing efficiency. Nevertheless, already with these experimental parameters RAP provides a higher efficiency and broader operation bandwidth compared to conventional  $\pi$  pulses, even under conditions initially optimized for  $\pi$  pulses. For a detailed investigation of RAP

rephasing, we refer the reader to our previous work on this subject [10]. To improve efficiencies as well as the robustness of the rephasing process, we now apply CAP sequences in our light storage experiment. The  $N$  single CAP pulses in a sequence exhibit the same Rabi frequency and chirp range as in the RAP experiments discussed above. As the experimental data show [see Fig. 2(a)] all CAP sequences clearly outperform  $\pi$  pulses and RAP; i.e., CAP yields high rephasing efficiencies over a broad operation range of pulse durations. For pulse durations beyond  $8$   $\mu\text{s}$ , the rephasing efficiency exhibits a stable plateau for all CAP sequences. As a pronounced feature, the diabatic couplings observed in RAP rephasing almost completely vanish. If we understood a CAP sequence simply as  $N$  subsequent RAP processes, we would expect far stronger diabatic couplings for CAP compared to RAP (as the perturbing effects of  $N$  subsequent, nonperfect RAP processes would be multiplied). However, the appropriately chosen phases in the CAP sequences reduce the diabatic couplings and lead to an improved robustness compared to RAP.

We note that theory predicts a higher efficiency in media of large inhomogeneous broadenings with increasing order  $N$  of the CAP sequences. We did not observe this effect in the plateau of high rephasing efficiencies at longer pulse durations. This is mainly due to the fact that the accuracy of our experimental data at a high signal level is not sufficient to resolve the expected improvement in efficiency for higher orders  $N$ . The theoretical maximal relative improvement in efficiency from an  $N = 3$  to an  $N = 5$  CAP sequence is of the order of only  $0.3\%$ . Already with the CAP sequence of order  $N = 3$  we operate at a rather high and stable efficiency.

Nevertheless, we clearly see the effect of higher order CAP sequences at short pulse durations, i.e., when the efficiencies are below the maximal values in the plateau regions. The higher the order  $N$ , the steeper and earlier the increase in the rephasing efficiency (i.e., the more quickly the CAP sequence approaches the region of high efficiency). As an example we note the CAP sequence with  $N = 7$ , which reaches the plateau of high rephasing efficiency (i.e., similar to the best performance observed in RAP for a single, specific pulse duration) at  $2 \mu\text{s}$  and maintains this high efficiency over the full range of longer pulse durations. In addition, we note the CAP sequence with  $N = 9$ , which yields the best efficiency of all rephasing sequences at  $2 \mu\text{s}$ .

As discussed above, our experimental parameters so far have permitted us to fairly (but not greatly) fulfill the adiabaticity criterion for RAP. With a chirp range of  $\Delta\nu = 600 \text{ kHz}$  the first adiabaticity criterion yielded  $2\pi\Delta\nu/\Omega_{\text{RF}} = 4.14$ . Under these imperfect conditions, CAP outperformed RAP. We apply now the larger chirp range of  $\Delta\nu = 900 \text{ kHz}$  while maintaining the Rabi frequency, yielding  $2\pi\Delta\nu/\Omega_{\text{RF}} = 6.21$ . Thus, we expect better adiabaticity in a larger operation bandwidth, especially at long pulse durations, i.e., fewer residual diabatic couplings. Figure 2(b) shows a comparison of the rephasing efficiencies by RAP and CAP in this case. We note that there are still some strong oscillations in the rephasing efficiency of RAP for shorter pulse durations. This becomes clear upon taking a look at the second adiabaticity criterion for RAP: The ratio  $\Omega_{\text{RF}}^2/R$  yields variations of between 0.07 and 3.67 for pulse durations of between 0.5 and  $25 \mu\text{s}$ . Thus, the second adiabaticity criterion for the specific case of short pulses is worse fulfilled compared to the case of the smaller chirp range of  $\Delta\nu = 600 \text{ kHz}$ . However, at long pulse durations both adiabatic criteria are better matched and lead to fewer diabatic couplings. The oscillations in the RAP rephasing efficiency damp out with increasing pulse duration and are about to approach a stable plateau. We note that, compared to the case of the smaller chirp range [see Fig. 2(a)] the maximal rephasing efficiency does not improve. This agrees with our expectation, as the larger chirp range only improves the adiabaticity, i.e., the convergence towards the maximal level.

We now apply CAP sequences of order  $N = 3, 5, 7$ , and  $9$ . Also, with this larger chirp range all CAP sequences outperform RAP in terms of robustness with regard to variations in the pulse duration. However, at short pulse durations (i.e., up to  $10 \mu\text{s}$ ), the lower order CAP sequences cannot compensate the lack of adiabaticity. In particular, the CAP sequence with  $N = 3$  shows a reduced rephasing efficiency at pulse durations in the range of  $2\text{--}12 \mu\text{s}$ . At these short pulse durations the rephasing efficiency significantly improves for higher order CAP sequences with  $N = 5, 7$ , and  $9$ . The larger the order, the steeper the progress towards the stable plateau of maximal rephasing efficiency. This clearly confirms the advantages of CAP to provide robust and efficient rephasing, even under imperfect adiabatic conditions.

To confirm our experimental results, we performed numerical simulations of the inversion dynamics in an inhomogeneously broadened two-level system, driven by RAP and CAP. Figures 2(c) and 2(d) show some results of the simulations, for chirp ranges of  $\Delta\nu = 600$  and  $900 \text{ kHz}$ , respectively. For

better comparison, the experimental data (symbols) are shown overlapping with the simulations (solid and dotted lines). The simulations fit the experimental data very well. All main features of the experiment are confirmed by the simulations. In order not to overload the graphs, we do not present calculations for CAP with  $N = 5, 7$ , and  $9$  here. Nevertheless, also our simulations for  $N = 5, 7$ , and  $9$  (not depicted here) fit the experimental data very well.

Above we have compared the performance of RAP and CAP under equal adiabaticity conditions. This required the same chirp rates and the same single-pulse durations in both techniques. Thus, the total pulse duration of the  $N$ -pulse CAP sequence was always longer than the RAP pulse. For a comparison under more practical conditions, it is also of interest to study the performance of RAP and CAP at the same total pulse duration and with optimal chirp rates for RAP or CAP chosen independently of each other. Though in this case the adiabaticity conditions are different for RAP and CAP, they correspond to a typical situation in an experiment: The total pulse duration is given, the Rabi frequency is kept fixed, and we optimize the remaining free parameter (i.e., the chirp rate or chirp range) to yield the highest rephasing (i.e., inversion) performance. Figure 3 depicts the results of this comparison, i.e., the rephasing efficiency for RAP and CAP (with  $N = 7$  single pulses as an example) vs the total pulse duration  $\tau_{\text{tot}}$ . We separated the full range of total pulse durations (i.e., from  $11$  to  $84 \mu\text{s}$ ) in our measurement into seven intervals. At the center of each interval we optimized the chirp range of the RAP pulses to provide the highest efficiency. The chirp rates in a RAP and the corresponding CAP sequence at the same total pulse duration are different. As the CAP sequence consists of  $N = 7$  single pulses with equal chirp, the chirp rate in CAP is typically higher, hence the adiabaticity conditions are typically better fulfilled for RAP. Thus, the comparison is very conservative. We note that to optimize RAP for different pulse durations, we had to vary the chirp range substantially. This is due to the fact that the adiabaticity condition for RAP varies for different pulse durations. CAP is far less sensitive to such variations of the adiabaticity. Therefore, we could essentially keep a fixed chirp range for CAP at an arbitrary total pulse duration. This feature already reveals the pronounced robustness of CAP compared to RAP.

The experimental data in Fig. 3(a) confirm the better performance of CAP also with regard to variation of the total pulse duration, in particular, at short pulse durations (i.e., for  $\tau_{\text{tot}} < 30 \mu\text{s}$ ). In this case, RAP still suffers very much from low adiabaticity and strong residual diabatic couplings. These show up as a low average efficiency and very pronounced oscillations of the rephasing efficiency vs the total pulse duration. CAP is far less affected by these residual diabatic interactions. Already at short pulse durations, the rephasing efficiency reaches and stays at a high level. The fluctuation in the RAP efficiency vs the total pulse duration is larger by a factor of  $4\text{--}5$  compared to CAP (see shaded areas in Fig. 3). As expected, at large total pulse durations the efficiencies of RAP and CAP are essentially the same. In this case, adiabaticity is well fulfilled for RAP and the inversion efficiency is maximal. There is nothing to be improved by CAP then. The data and the corresponding simulation [see Fig. 3(b)] confirm the same behavior of CAP, as already observed for comparison with

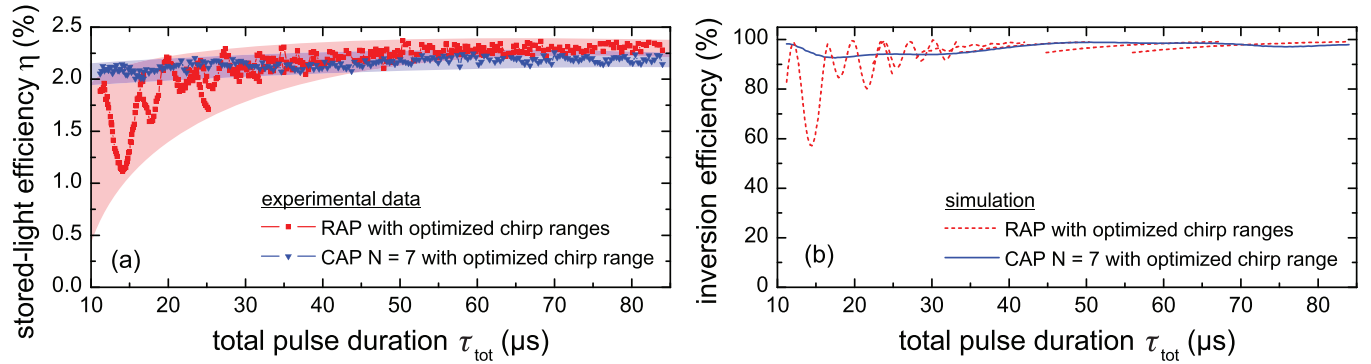


FIG. 3. (Color online) Stored-light efficiency  $\eta$  due to rephasing by RAP and CAP (with  $N = 7$  pulses) vs total pulse duration  $\tau_{\text{tot}}$ . The Rabi frequency is kept fixed at  $\Omega_{\text{RF}} = 2\pi \times 145$  kHz. All pulses have a rectangular temporal shape of the intensity. The chirp ranges for RAP and CAP are optimized independently of each other: for RAP it ranges from roughly 0.6 MHz for short pulse durations to 3.2 MHz for long pulse durations, and for CAP the range is 0.5 MHz for all total pulse durations. (a) Experimental data. Shaded areas indicate variations in the rephasing efficiency. (b) Simulations.

regard to the single-pulse duration (see Fig. 2). CAP permits high efficiencies as well as robustness with regard to fluctuations of experimental parameters, in particular, when RAP does not yet work well (i.e., at a low adiabaticity, e.g., due to experimental limitations in the pulse duration, Rabi frequency, or chirp rate).

### B. CAP efficiency vs static detuning

In the above section we have discussed the operation range of  $\pi$  pulses, RAP, and CAP with regard to variations in the pulse duration. However, the pulse duration (or pulse area) is only one experimental parameter to be maintained. In addition, there might also be variations and fluctuations of the transition frequency (e.g., as in inhomogeneously broadened media) or variations of the carrier frequency of the driving radiation pulse (e.g., if the radiation source exhibits frequency drifts). To cope with such frequency fluctuations, the spectral bandwidth of the driving processes must be as large as possible. Also, in this case, RAP and CAP will offer broader operation bandwidths compared to  $\pi$  pulses. However, CAP was initially not meant to compensate variations of the static detuning. In other words, the phases as listed in Table I are optimal solutions with regard to variations in the pulse duration (or pulse area) but not the static detuning. It is of interest to know how well CAP will work, compared to RAP, also with regard to variations of the static detuning  $\Delta$ . We therefore vary the center frequency of the driving RF pulses, which leads to an asymmetry of the linear chirp around the resonance frequency of the system.

Figures 4(a)–4(d) show the experimental results and simulations for RAP pulses and CAP sequences, i.e., the rephasing efficiency vs the static detuning  $\Delta$  of the carrier frequency of the driving RF pulses. All other parameters were kept fixed, i.e., Rabi frequency  $\Omega_{\text{RF}} \approx 2\pi \times 145$  kHz and chirp range  $\Delta\nu = 900$  kHz. For the first measurement we chose the single-pulse duration  $\tau = 4 \mu\text{s}$  [see Fig. 4(a)]. In this case the RAP rephasing efficiency reaches a first maximum [compare with Fig. 2(b)]. However, at such short pulse durations RAP does not work very well because of the large residual diabatic couplings. In this case, the relevant quantity in the second adiabaticity criterion yields only  $\Omega_{\text{RF}}^2/R = 0.6$ , which is too low for adiabatic evolution. The (red) squares in Fig. 4(a) show

the variation of the stored-light efficiency when we vary the static detuning of the RAP pulse. As expected, the efficiency exhibits a maximum at  $\Delta = 0$  kHz, i.e., with a symmetric chirp around the relevant RF transition. At increasing static detuning  $\Delta$  the efficiency gradually decreases, and it approaches 0 at  $\pm 400$  kHz. This is mainly due to the fact that at a static detuning of  $\Delta = \pm 400$  kHz and a chirp range of  $\Delta\nu = 900$  kHz, the chirp is very asymmetric around the resonance and the driving pulse hardly meets the resonance any more. Thus, the bandwidth of the RAP process is roughly 200 kHz (FWHM). To compare with CAP, we now monitor the variation of CAP stored-light efficiency vs static detuning at single-pulse durations of  $\tau = 4 \mu\text{s}$ . Figure 4(a) shows the results for CAP sequences of orders  $N = 3, 5, 7$ , and 9. The efficiencies for all CAP orders feature quite complicated, periodic structures. As expected, at resonance (i.e.,  $\Delta = 0$  kHz) all CAP sequences exhibit a higher rephasing efficiency compared to RAP [see also Fig. 2(b) at  $4 \mu\text{s}$ ]. Already for rather small static detunings  $\Delta$  the efficiency quickly decreases and increases again. As an example, the efficiency for CAP sequences of orders  $N = 5$  and  $N = 9$  drops to almost 0 at  $\Delta \approx \pm 100$  kHz and shows prominent sidebands at  $\Delta \approx \pm(220-250)$  kHz, with efficiencies on a similar level as on resonance. Thus, in contrast to RAP, CAP enables rephasing also at static detunings larger than  $\pm 400$  kHz. However, it is hard to define and compare the spectral bandwidth of RAP and CAP from the data in Fig. 4(a), as the two processes exhibit very different spectral shapes. It would be a matter of debate whether CAP provides a small improvement in the spectral bandwidth compared to RAP under conditions of low adiabaticity.

We now repeat the experiment at the longer single-pulse duration of  $\tau = 21 \mu\text{s}$ , while keeping the Rabi frequency and chirp range as before. Now the second adiabaticity criterion is better fulfilled, as  $\Omega_{\text{RF}}^2/R = 3.1$ . Thus, adiabatic passage processes will suffer far less from residual diabatic couplings. As we see in Fig. 2(b), both RAP and CAP yield high and comparable efficiencies on resonance. The spectral bandwidth of RAP increases to roughly 600 kHz (FWHM), if we ignore some minor oscillations for static detunings between  $\pm 200$  kHz. As in the previous experiment with short pulses, RAP ceases to operate around  $\pm 400$  kHz. The CAP sequences

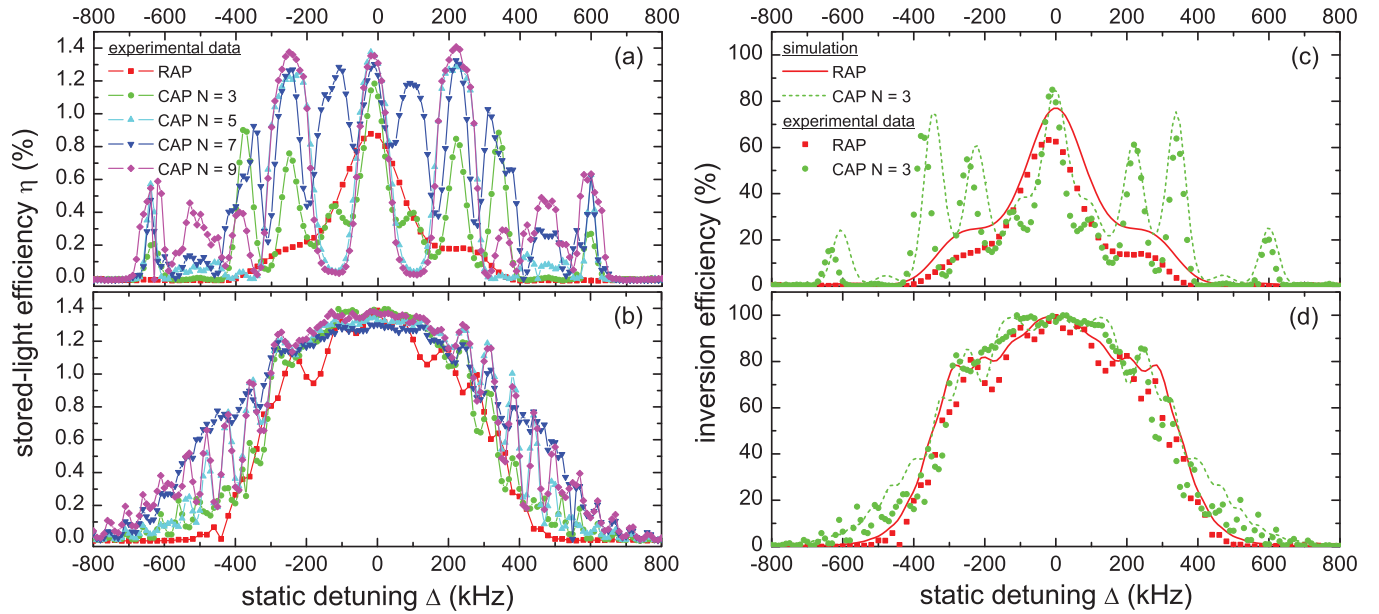


FIG. 4. (Color online) Stored-light efficiency  $\eta$  due to rephasing by RAP or CAP vs static detuning  $\Delta$ . In the case of CAP we apply sequences of  $N = 3, 5, 7,$  and  $9$  single pulses. The Rabi frequency is  $\Omega_{\text{RF}} = 2\pi \times 145$  kHz. The chirp range is fixed at  $\Delta\nu = 900$  kHz. All pulses have a rectangular temporal shape of the intensity. (a) Experimental data for a single-pulse duration (for RAP and CAP) of  $\tau = 4$   $\mu\text{s}$ . (b) Experimental data for a single-pulse duration (for RAP and CAP) of  $\tau = 21$   $\mu\text{s}$ . Lines along the experimental data are guides for the eye only. (c, d) Simulations (solid and dotted lines) and corresponding experimental data (filled squares, RAP; filled circles, CAP) at single-pulse durations of (c)  $\tau = 4$   $\mu\text{s}$  and (d)  $\tau = 21$   $\mu\text{s}$ . We note that in the simulations we depict the calculated inversion efficiency instead of the measured stored-light efficiency (which both are proportional to each other).

still show some oscillations in the stored-light efficiency vs static detuning, in particular, in sequences with  $N = 5$  and  $N = 9$  pulses. However, the oscillations are strongly damped. Essentially all CAP sequences yield an improved bandwidth compared to RAP. As an example, the CAP sequence of order  $N = 7$  exhibits a spectral bandwidth of almost 1000 kHz (FWHM). We also note the smooth behavior of all CAP sequences in the range of  $\pm 200$  kHz. In this range, RAP shows stronger oscillations of the rephasing efficiency, while CAP yields very smooth variation at a high level. Thus, our experimental results show that, under conditions of adiabatic evolution, CAP provides an improved spectral bandwidth compared to RAP, though CAP was not optimized for this case.

We again performed numerical simulations in an inhomogeneously broadened system. Figures 4(c) and 4(d) show the simulations for a single-pulse duration of  $\tau = 4$   $\mu\text{s}$  and 21  $\mu\text{s}$ , respectively. The simulation of RAP is depicted by solid (red) lines; the corresponding experimental data, by filled (red) squares. The simulation [dashed (green) lines] and experimental data [filled (green) circles] for the CAP sequence with  $N = 3$  are also shown for comparison. The simulations clearly confirm the experimental results.

## V. CONCLUSION

We have demonstrated the experimental implementation of CAP, which was recently proposed for efficient and robust inversion of the population distribution in a two-level quantum system. CAP serves to reduce residual diabatic perturbations, which always occur in realistic implementations of RAP. Essentially, CAP is a composite version of RAP, driven

by sequences of RAP pulses with appropriately defined relative phases. These phases serve as control parameters to optimize the adiabatic passage process. To demonstrate and systematically study CAP, we applied it for inversion or rephasing of atomic coherences in a rare-earth ion-doped solid, driven by RF radiation pulses. The atomic coherences were optically prepared and read out by EIT. In our experiments we compared rephasing by conventional  $\pi$  pulses, RAP, and several CAP sequences. In particular, we studied the variation of the rephasing efficiency when we systematically changed the pulse duration or the static detuning of the driving RF pulses. In the experimental data, the residual diabatic couplings in RAP are clearly visible as strong oscillations of the stored-light efficiency (i.e., RAP rephasing efficiency) vs the single-pulse duration. Depending on the exact choice of the single-pulse duration, the RAP rephasing efficiency oscillates by more than 50%. Under the same experimental conditions (i.e., without changing the intensity or chirp range of the single RAP pulses in the sequence), CAP strongly reduces the effect of residual diabatic couplings. The oscillations in the stored-light efficiency vs single-pulse duration almost completely vanish. As a result, the efficiency of rephasing by CAP remains at a high level, irrespective of the exact choice of the pulse duration. Thus, the operation bandwidth of CAP with regard to variations in the pulse duration is way beyond RAP. This permits efficient rephasing by CAP even under conditions of rather small adiabaticity, which does not yet allow efficient and stable operation by conventional RAP. Moreover, we also investigated the variation of the rephasing or inversion efficiency with regard to changes in the static detuning of the driving pulses. Though CAP

was initially not designed also to compensate variations of the static detuning, it operates very well in this case too. Numerical simulations of the coherent inversion dynamics in an inhomogeneously broadened two-level system confirm all our experimental data. The demonstration of CAP will be of interest for applications in quantum optics and related fields, which require techniques for robust and efficient manipulation of population distributions or atomic coherences.

### ACKNOWLEDGMENTS

The research leading to these results received funding from the Deutsche Forschungsgemeinschaft, the Volkswagen Foundation, the Alexander von Humboldt-Foundation, and the People Programme (Marie Curie Actions) of the European Union's Seventh Framework Programme FP7/2007-2013/ under REA Grant No. 287252.

- 
- [1] N. V. Vitanov, T. Halfmann, B. W. Shore, and K. Bergmann, *Annu. Rev. Phys. Chem.* **52**, 763 (2001).
  - [2] M. M. T. Loy, *Phys. Rev. Lett.* **32**, 814 (1974).
  - [3] J. Klein, F. Beil, and T. Halfmann, *J. Phys. B* **40**, S345 (2007).
  - [4] K. Bergmann, H. Theuer, and B. W. Shore, *Rev. Mod. Phys.* **70**, 1003 (1998).
  - [5] B. T. Torosov, S. Guérin, and N. V. Vitanov, *Phys. Rev. Lett.* **106**, 233001 (2011).
  - [6] B. T. Torosov and N. V. Vitanov, *Phys. Rev. A* **83**, 053420 (2011).
  - [7] M. H. Levitt, *Prog. NMR Spectrosc.* **18**, 61 (1986).
  - [8] M. Fleischhauer, A. Imamoglu, and J. P. Marangos, *Rev. Mod. Phys.* **77**, 633 (2005).
  - [9] A. V. Turukhin, V. S. Sudarshanam, M. S. Shahriar, J. A. Musser, B. S. Ham, and P. R. Hemmer, *Phys. Rev. Lett.* **88**, 023602 (2001).
  - [10] S. Mieth, D. Schraft, T. Halfmann, and L. P. Yatsenko, *Phys. Rev. A* **86**, 063404 (2012).
  - [11] M. F. Pascual-Winter, R. C. Tongning, R. Lauro, A. Louchet-Chauvet, T. Chanelière, and J.-L. Le Gouët, *Phys. Rev. B* **86**, 064301 (2012).
  - [12] E. L. Hahn, *Phys. Rev.* **80**, 580 (1950).
  - [13] H. Y. Carr and E. M. Purcell, *Phys. Rev.* **94**, 630 (1954).
  - [14] R. Lauro, T. Chanelière, and J.-L. Le Gouët, *Phys. Rev. B* **83**, 035124 (2011).
  - [15] G. Heinze, C. Hubrich, and T. Halfmann, *Phys. Rev. Lett.* **111**, 033601 (2013).
  - [16] M. Nilsson, L. Rippe, S. Kröll, R. Klieber, and D. Suter, *Phys. Rev. B* **70**, 214116 (2004).
  - [17] F. Beil, J. Klein, G. Nikoghosyan, and T. Halfmann, *J. Phys. B* **41**, 074001 (2008).